Energy

SOLAR

PROTOTYPE DESIGN OF AN ADVANCED CERAMIC RECEIVER

Final Report

April 1984

Work Performed Under Contract No. AC03-83SF11938

Martin Marietta Aerospace
Denver Aerospace
Denver, Colorado

Technical Information Center
Office of Scientific and Technical Information
United States Department of Energy

DISCLAIMER

Available from the National Technical Information Service, U. S. Department of Commerce, Springfield, Virginia 22161.

Price: Printed Copy A03
Microfiche A01

Codes are used for pricing all publications. The code is determined by the number of pages in the publication. Information pertaining to the pricing codes can be found in the current issues of the following publications, which are generally available in most libraries: *Energy Research Abstracts (ERA); Government Reports Announcements* and Index (*GRA* and I); *Scientific and Technical Abstract Reports (STAR);* and publication NTIS-PR-360 available from NTIS at the above address.

Printed in the United States of America
USDOE Technical Information Center, Oak Ridge, Tennessee

MCR-84-537
(DE84009695)
Distribution Category UC-62d

MCR-84-537
DOE/SAN Contract
DE-AC03-83SF11938

Final
Report

April 1984

PROTOTYPE DESIGN OF AN ADVANCED CERAMIC RECEIVER

MARTIN MARIETTA AEROSPACE
DENVER AEROSPACE
P.O. Box 179
Denver, Colorado 80201

FOREWORD

This report is submitted by the Martin Marietta Corporation to the Department of Energy, San Francisco Operations Office, in accordance with the provisions of the contract numbered DE-AC03-83SF11938. This final report consists of a single volume and incorporates the data and information which would have been appropriate for presentation in a Topical Report. Dr Keith A. Rose, Fossil, Geothermal & Solar Energy Programs Division, Department of Energy, San Francisco Operations Office, provided the technical direction for this activity. He was assisted locally by Dr. David Harley Johnson, Solar Thermal Research Branch, Solar Energy Research Institute, Golden, Colorado.

TABLE OF CONTENTS

I. INTRODUCTION

Solar thermal central receiver power systems consist of a field of two-axis tracking mirrors, called heliostats, that reflect solar energy into a receiver mounted on a tower. Solar energy is collected by the receiver's working fluid and is then used to produce electric energy or for process heat. Several types of working fluids are candidates for commercial system, including molten salt, water/steam, liquid metals, and gases. Gas receivers are generally considered the most appropriate type for high temperature applications with outlet temperatures up to about 1100°C (2012°F). The purpose of the activities described in this report is to investigate an advanced gas receiver design concept.

A. Background

The advanced gas receiver design concept illustrated in Figure 1 was conceived at Martin Marietta in 1981. This concept utilizes a translucent ceramic tube packed with a solar absorbing, porous material. A gas is pumped through the tube and is heated to a high temperature by direct solar energy incident on the tube surface. The basic energy exchange mechanisms are the transfer of the incoming solar flux through the translucent tube, the absorption of the solar energy by the packing material, and the convective transfer of the absorbed solar energy from the packing material to the gas.

Martin Marietta began developing the translucent ceramic tube receiver in 1981. The activity in 1981 was internally funded through the Independent Research and Development (IR&D) program. The tasks performed included radiation property tests of the alpha-alumina material and a proof-of-concept test of the tube configuration shown in Figure 1. The radiation property tests resulted in solar transmissivity values for the alpha-alumina of 60%. The proof-of-concept performance tests were conducted at a maximum solar flux of 9.5 watts/cm^2 (30,000 Btu/hr-ft^2). A flux level of this amount is small relative to fluxes consistent with a commercial central receiver, however, the tests indicated that the approach was viable and provided basic heat transfer data. Using these data it was possible to correlate an analytical model of the absorber tube and then extrapolate performance estimates to high solar flux levels. This extrapolation indicated that the concept was a reasonable approach for producing high gas temperatures with a solar central receiver. Our conviction that the translucent ceramic receiver concept was competitive relative to other gas receiver concepts lead us to propose this concept in DOE's Innovative Research Program in Solar Thermal. The subject of this report is the activity we have performed through a contract in the Innovative Research Program.

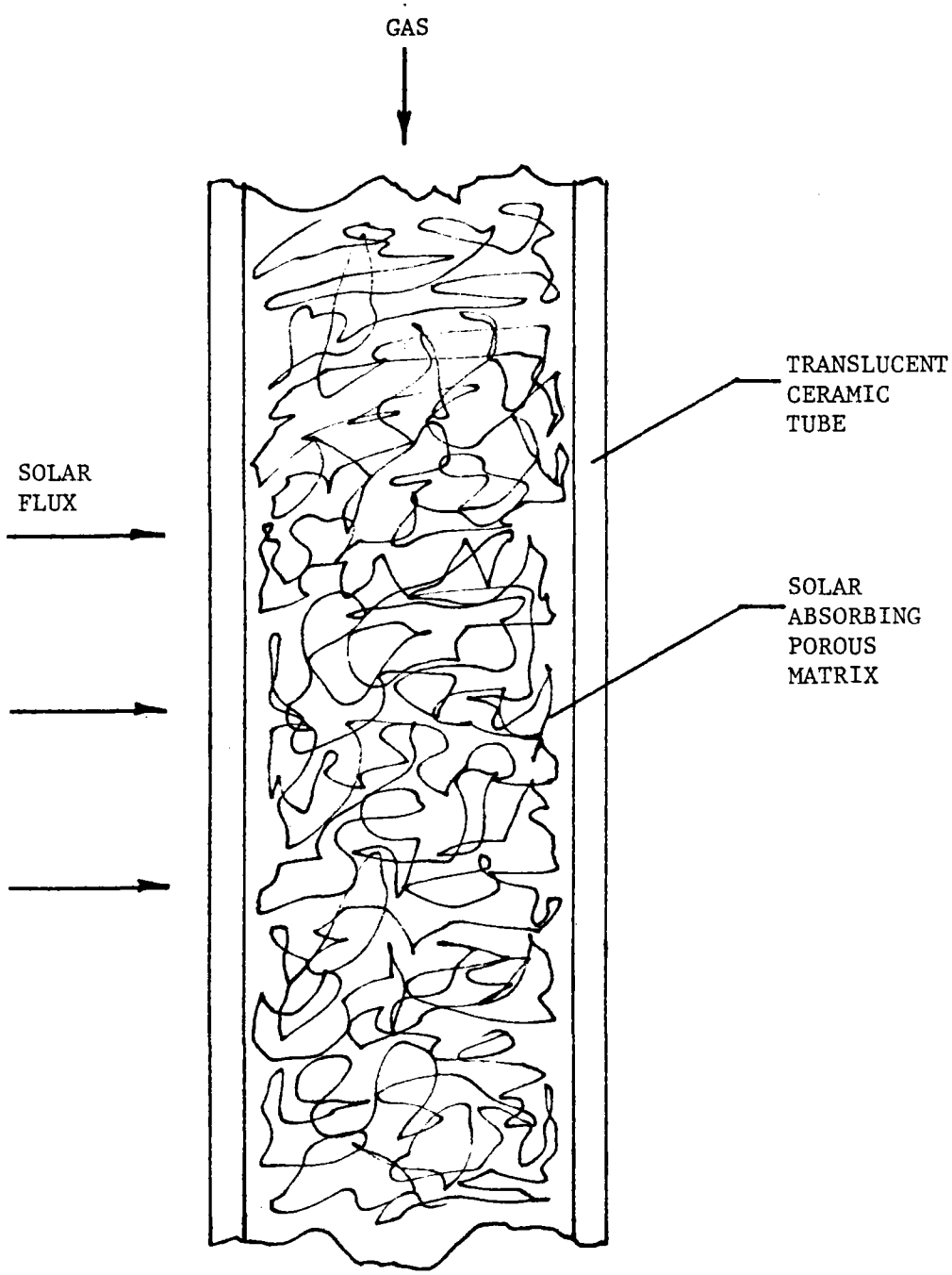

Figure 1 Basic Concept

B. Approach

The approach taken for this activity was to develop a conceptual design of a commercial size receiver, investigate critical design elements of the commercial receiver, develop a preliminary design of a prototype, and identify the appropriate facility for testing the prototype. In order to develop the conceptual design of the commercial size receiver a thermo/hydraulic numerical model of the tube was devised. This model yields predictions of the thermal performance of the tube along with estimates of the tube pressure drops. A detailed description of the model is given in section III A of this report. Using the model it was possible to establish an optimum tube diameter and length for a commercial size receiver. With the tube dimensions known it was then possible to perform design studies to determine tube stresses and attachment schemes.

The approach taken for establishing a conceptual design of the receiver/heliostat field configuration was based on the use of the DOMAIN program. This microcomputer program was developed by Martin Marietta and provides estimates of heliostat field boundaries, flux distributions, and aiming strategy requirements. The results of this program have been shown to be in agreement with the more exact (and more expensive) TRASYS program.

In the materials area thermal shock tests were performed by the Advanced Components Test Facility at the Georgia Institute of Technology. Properties of the selected tube material (alpha-alumina) were determined from texts and vendor data. Alpha-alumina availability information was obtained by discussions with personnel from General Electric, Coors Porcelain, and Ceramatec.

II. SUMMARY

This section provides a summary of the work performed relative to each of the contract Statement of Work tasks.

A. Conceptual Design of a Commercial Size Receiver.

The baseline size of the commercial receiver was chosen to be $50MW_t$. This rating was picked based on an evaluation made by Stone and Webster of solar assisted syn fuel plants. Even though their finding stated that $50MW_t$ was on the low end of economically viable sizes, this size was chosen because it conforms to the size used in the comparative study by Sandia, "Solar Central Receiver High Temperature Process Air Systems," SAND 82-8254, February 1983.

The inlet and outlet gas conditions for the baseline receiver were taken as representative values and based on the syn fuel system under study at Stone and Webster. These conditions are an inlet pressure of 10^6 Pa (145 psia) an inlet temperature of 538°C (1000°F), and an outlet temperature of 1093°C (2000°F).

Nitrogen was assumed to be a representative gas. The thermophysical properties of nitrogen were allowed to vary with temperature in all the analysis performed on this contract.

The maximum inlet gas velocity to the absorber was limited to 30.5 m/s (100 ft/sec). This value is given as the limit for good design practice in, "Heat Exchanger Design," by Fraas and Ozisik, p. 135. The gas velocity does increase considerably above 30.5 m/s (100 ft/sec) as it travels through the absorber tubes. It is assumed that this relatively high gas velocity will not present a problem in straight tubes. The maximum temperature difference, front to back of tubes, at any axial location along the tubes was set at 93°C (200°F). This value was based on an estimate of thermal stresses caused by temperature differences across the tubes.

Using the criteria given above, parametric analysis were performed on the receiver tubes varing the tube diameter, inlet gas velocity, and incident flux. The results of the analysis yielded a receiver tube design of 10.2 cm (4 in.) outside diameter, an inlet velocity of 30.5 m/s (100 ft/sec), and an average incident flux of 86.8 W/cm^2 (275000 $Btu/hr-ft^2$). The temperature rise of 556°C (1000°F) across the receiver is achieved by each tube, thus there is a single pass of the gas across the absorber. Ninety vertical tubes are used to collect the 50MW required by the system.

The cavity design is governed by the image size of the sun from the individual heliostats. This means that the solar flux levels acceptable relative to the tube thermo/hydraulic performance is greater than is obtainable from the heliostat field considering a reasonable depth of the

cavity. A compromise was, therefore, taken and the flux levels were reduced below maximum possible values in order to match the level with a practical cavity design. This compromise resulted in the cavity design shown in Figure 2. The cavity is designed to provide as deep an enclosed space as possible around the receiver absorber panel. This provides a high temperature dead air space for the receiver and will tend to minimize convection and emitted radiation losses. Figure 3 illustrates the layout configuration of the receiver tubes. The ceramic tubes which form the absorber panel are attached to steel tubes on the inlet and outlet of the absorber. The size of the attachment/coupling prevent the ceramic tubes from being placed side-by-side. They are staggered in two rows so that when viewed from the heliostat side they appear to form a solid surface. The back row of tubes will receive less solar energy than the front row (closest to the heliostats) because of partial shadowing. Also, there will be a flux distribution across the absorber with the higher fluxes toward the middle. Therefore, the tubes will be divided into six control zones as shown on Figure 3. The tubes in each control zone will be connected by a manifold on the inlet and controlled by a single value. The control of the outlet temperature will be easily accomplished due to the extremely short dwell time of the gas as it passes through the absorber tubes. Table 1 lists the major design characteristics of the commercial size receiver.

B. Investigation of Critical Design Elements

The most critical design elements of the commercial size receiver are the attachments of the ceramic tubes and the coupling of the ceramic tubes to the metallic tubes which provide the flow passages for the system other than the receiver absorber tubes. An illustration of the attachment/coupling design is given in Figure 4. The lower attachment/coupling is similar to the design proposed by Black and Veatch for their opaque ceramic tube receiver. This approach has been analyzed and tested by AiResearch under the EPRI contract, "Analysis of Thermal and Mechanical Stresses in the Ceramic Seal of the 1-MW (th) Bench-Model Solar Receiver", (AP-2267, Research Project 475-9). The upper attachment/coupling is a one-stage labyrinth type seal which allows unconstrained thermal growth along the axis of the tube. Also, with an initial 0.0157 mm (0.004 in,) gap clearance, thermal distortions will not cause interference with this seal arrangement. Details of the attachment/coupling design are given in section III-C.

C. Preliminary Design of a Prototype Reveiver

A sketch of a prototype receiver is given in Figure 5. The prototype consists of six tubes which are the same length and diameter of the commercial size receiver. Also, note that the center front row tube and center back row tube have adjacent tubes just as they would in the commercial size receiver. Therefore these tubes would experience the same type radiation and convection environments they would in a commercial receiver.

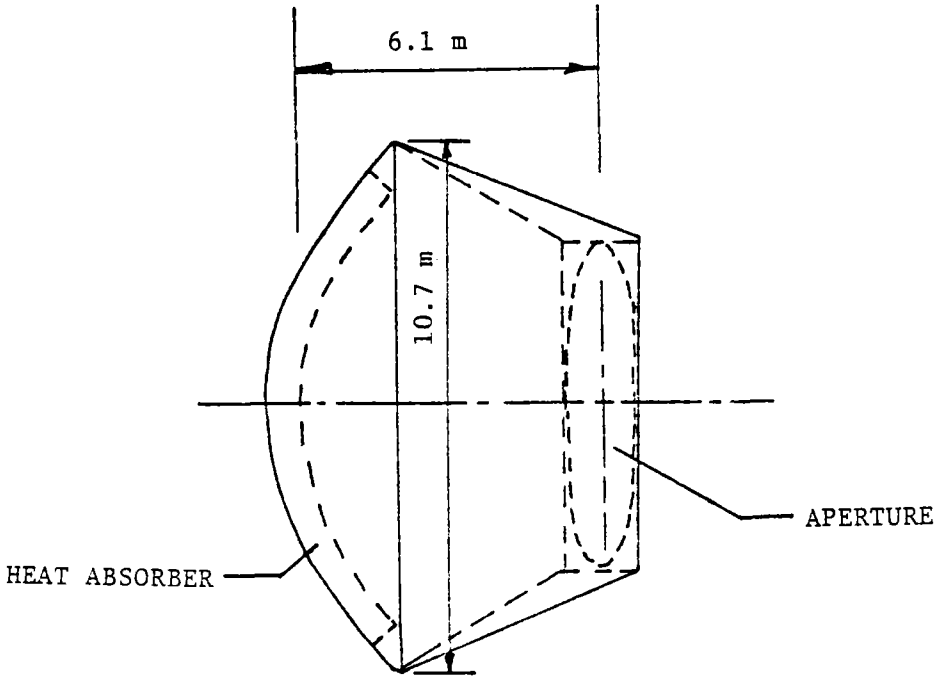

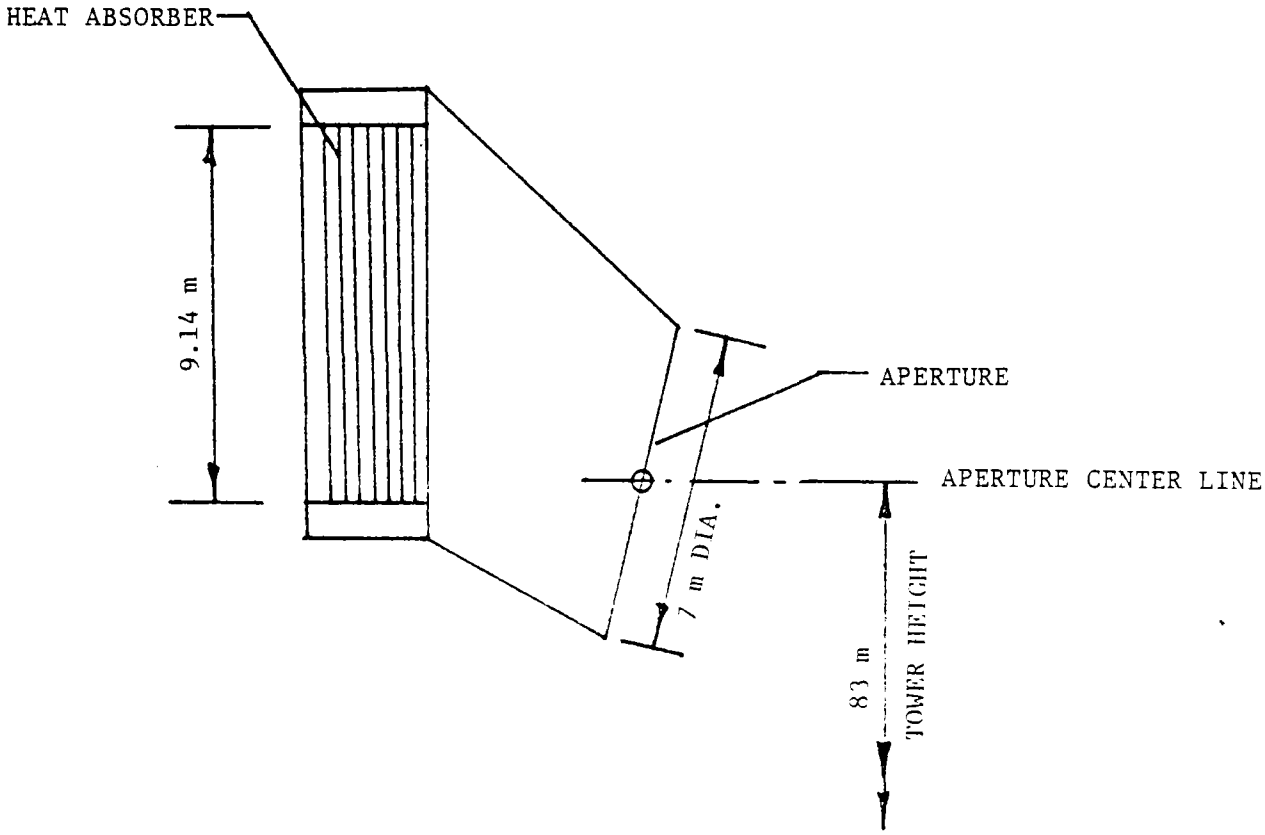

Figure 2 Commercial Scale Receiver Cavity Design

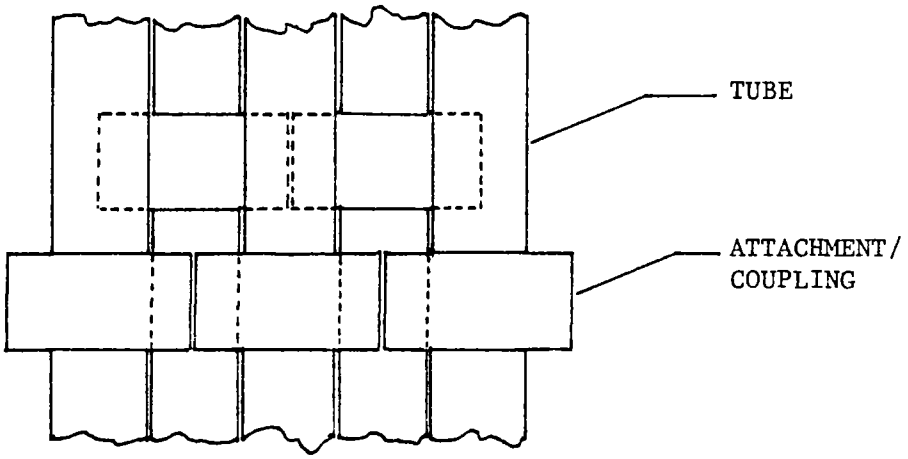

FRONT VIEW

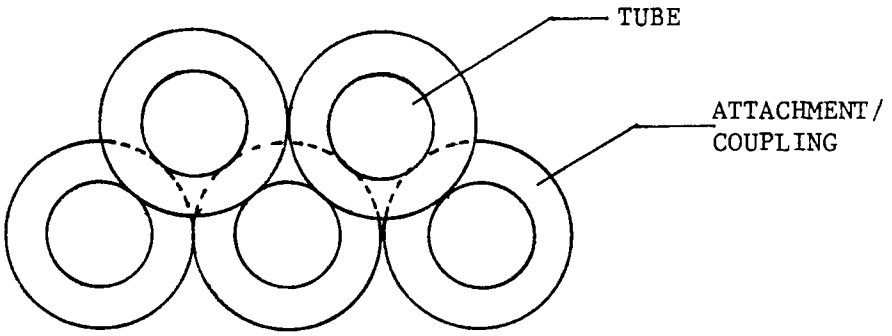

TOP VIEW

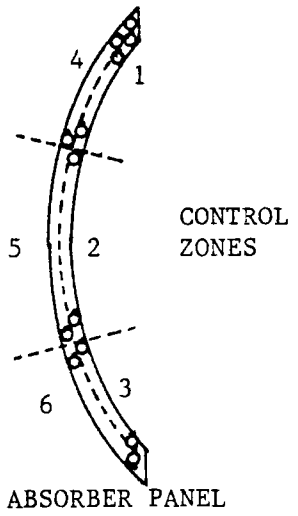

Figure 3 Receiver Tube Arrangement

Table I Characteristics of Commercial Receiver Design

Absorbed Power	50 MWt
Number of Tubes	90
Tube Size	
Outside Diameter	10.16cm (4 in.)
Inside Diameter	9.21cm (3.625 in.)
Length	8.53m (28 ft)
Absorber Size	7.62 x 9.14m (25 x/30 ft)
Average Flux	8.68 w/cm^2 ($275,000$ BTU/hr-ft^2)
Inlet Velocity	30.48 m/s (100 ft/s)
Inlet Pressure	10^6 Pa (145 psia)
Pressure Drop	9.72×10^4 Pa (14.1 psi)
Tube Front to Back Temp Difference	93.9°C (169°F)
Mass Rate of Flow/Tube	3034 kg/hr (6689 lb/hr)
Leakage Rate from Seals	4.3% of flow
Work of Compression to Overcome Pressure Loss	4.3% of heat absorbed
Efficiency (Heat Absorbed/ Incident Flux)	84%

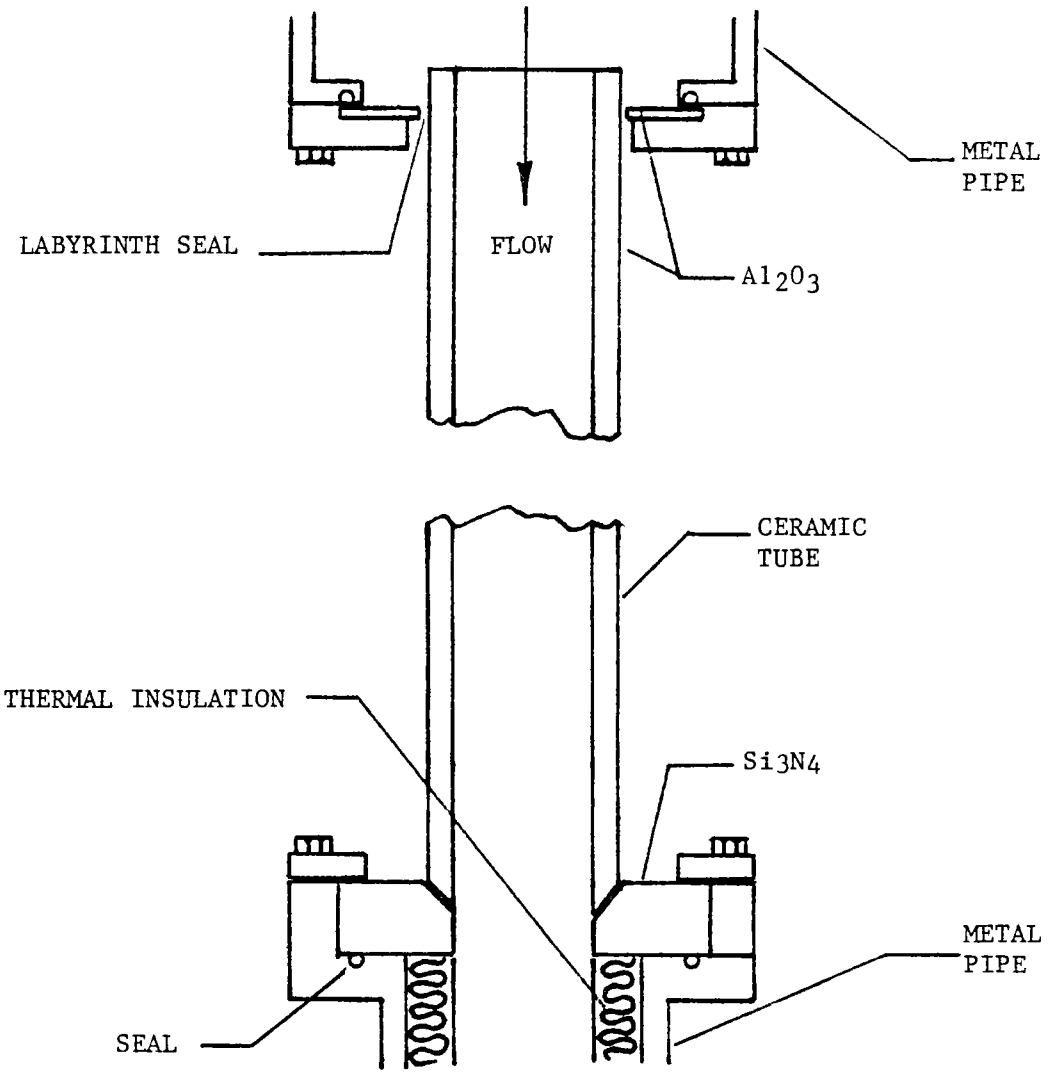

Figure 4 Baseline Design for Receiver Tube Attachment/Coupling

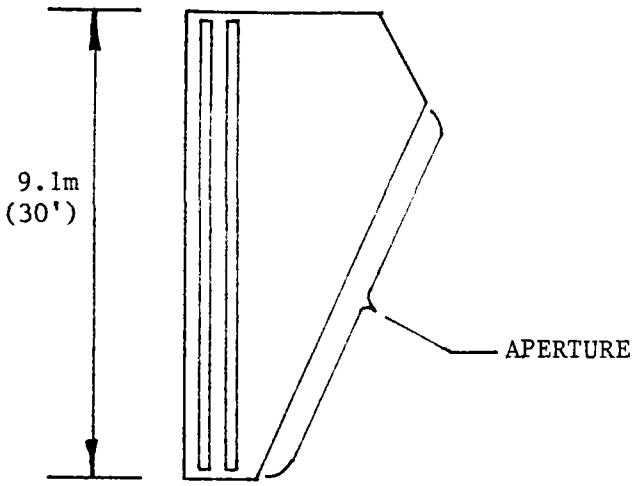

SIDE VIEW

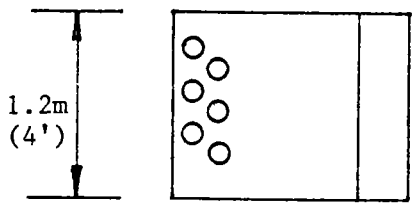

TOP VIEW

Figure 5 Prototype Receiver Design

The prototype design as shown in Figure 5 would be the most reasonable configuration for developing our translucent tube receiver concept. However, as will be discussed in detail in Section IV, it does not appear that alpha-alumina tubes of this length will be available in the foreseeable future. Therefore, we suggest as an alternate the prototype design shown in Figure 6. This design utilizes alpha-alumina tubes which are currently available from Coors Porcelain. These 10.2cm (4 inch) diameter tubes are the same diameter as those used for the commercial size receiver. The length of the heating section, however, will be 0.61 m (2 ft) instead of 7.6 m (25 ft). This length will provide temperature changes of the gas of about 27°C (80°F) and pressure drops of around 7777 Pa (1.12 psi). These magnitudes of temperature and pressure changes are certainly reasonable for measurement purposes. Therefore, this size prototype will yield basic thermo/hydraulic data at the same solar radiation flux level and with the same ceramic tube diameter as the commercial size receiver.

D. Identification of Solar Test Facility

In our opinion the proper test facility for testing the prototype receiver would be the Central Receiver Test Facility in Alburquerque, New Mexico. This facility is the only U.S. solar facility which can provide the necessary power input of about 3.3 MW. Also the north field layout of the heliostats is appropriate for the type cavity we envisioned for the prototype and commercial designs. As stated earlier, it appears unlikely that 7.6 m (25 ft) alpha-alumina tubes will be available in the foreseeable future. Therefore, the alternate prototype receiver is the design which is the likely candidate for testing. Since this size receiver requires a much lower power level than the "full scale" prototype, it is recommended that the alternate prototype be tested at the Advanced Components Test Facility at the Georgia Institute of Technology.

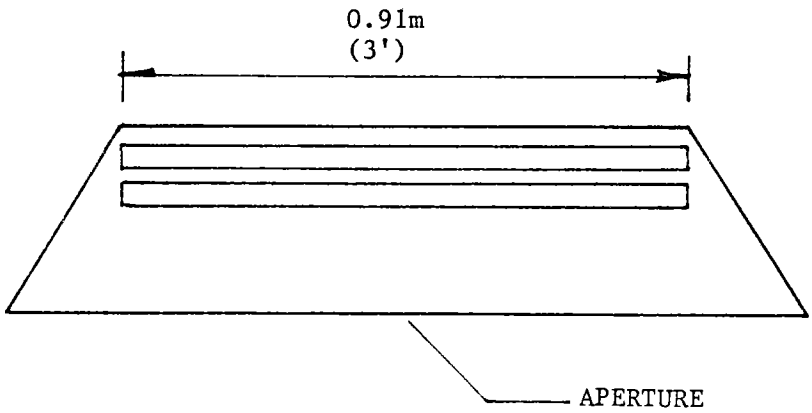

SIDE VIEW

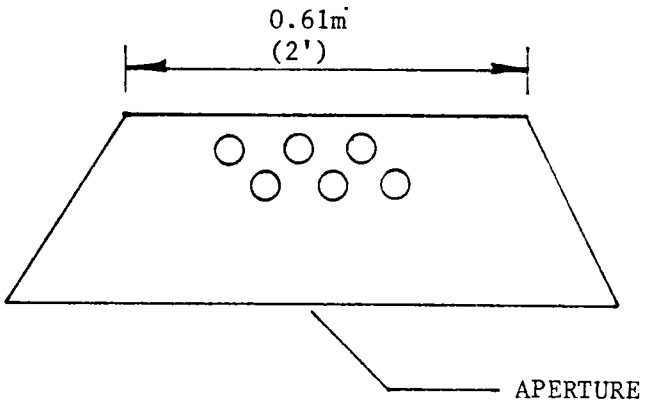

SIDE VIEW

Figure 6 Alternate Prototype Receiver Design

III. ANALYSIS AND DESIGN

Details of the thermo/hydraulic analysis, heliostat analysis, and detail design studies will be presented in this section of the report.

A. Thermo/Hydraulic Analysis

The behavior of the gas as it flows through the absorber tubes of the receiver is influenced by compressible effects. In order to understand the relationship between the thermal and hydraulic aspects of the problem for a compressible fluid, a simplified model of the absorber tube was investigated. The major differences in this model and the numerical model that was eventually devised for predicting tube performance were that for the simplified model the incoming solar energy was absorbed directly into the gas and the pressure drop was described by a pipe flow relationship. This relationship was modified to simulate a packed bed condition. For the more detailed model which was used to predict performance the solar energy is absorbed by the packing and then transferred to the gas via convection. Also the pressure drop calculation in the detailed model are written for a packed bed situation instead of a pipe flow condition. These differences were made for the initial analysis in order to simplify the calculations. However, the similarity of the initial model is certainly close enough to the actual receiver tube to provide an insight into the problem and to guide the development of the detailed numerical model.

The governing equations for the simplified model are as follows.

Energy Equation

$$(1) \qquad \frac{D\,dx\,q}{m} = h + \frac{V\,dV}{g_c J}$$

Momentum Equation

$$(2) \qquad dP + \frac{f\,V^2\,dx}{2\,g_c\,D} + \frac{m\,dv}{A\,g_c} = 0 \quad , \; f = .184/Re^{0.2}$$

Continuity Equation

$$(3) \qquad \rho VA = m$$

Ideal Gas Equations

$$(4) \qquad P = \rho RT$$

$$(5) \qquad dh = C_p\,dT$$

where:

A=	tube cross sectional area
D=	Tube diameter
h=	gas enthalpy
C_p=	gas specific heat
f=	friction factor
gc=	unitary constant
m=	mass rate of flow
J=	mechanical equivalent of heat
q=	heat input
V=	gas velocity
x=	axial distance along tube
P=	gas pressure
ρ =	gas density
Re=	$\frac{\rho VD}{\mu}$ = Reynolds Number
μ =	gas viscosity
R=	gas constant
T=	gas temperature

The equations were solved simutaniously by re-writing the equations in a numerical form and evaluating using a mini computer. A sample problem was solved with the following inlet conditions:

Temperature	= 537.7°C (1000°F)
Pressure	= 6.89 x 10^5 Pa (100psia)
Velocity	= 30.5 m/s (100 ft/sec)
Solar flux	= 126.2 w/cm^2 (400,000 Btu/hr -ft^2).
Tube transmissivity	= 0.6
Tube Diameter	= 0.533 cm(.21 inches)

At 15 inches down stream of the inlet, the conditions were computed to be:

Temperature	= 1201.1 °C (2194.1°F)
Pressure	= 6.7903 x 10^5 Pa (98.485 psia)
Velocity	= 56.27 m/s (184.6 ft/sec)

If in equation (1), the energy equation, the enthalpy term is compared to the kinetic energy term (first and second terms on the right hand side of the equation) it is found that the kinetic energy is only about 0.14% of the enthalpy term. Therefore, it is reasonable to neglect the kinetic energy term. This is significant since it decouples the energy equation from the momentum equation. This allows the evaluation of the frictional and velocity pressure drops (the second and third terms of the momentum equation, respectively) separately. This was done and the resulting total pressure drop was within 1.2% of the pressure drop computed by solving the coupled equations. The important conclusions are that the energy equation can be solved neglecting the kinetic energy term and the pressure drop can be estimated accurately by evaluating the frictional and velocity heads separately. These varified simplifying assumptions are used in developing the generalized numerical techniques.

The generalized computer program which was developed for predicting the performance of the absorber tubes utilized a transient execution routine of the Martin Marietta Interactive Thermal Analysis System (MITAS) program. The transient routine was used, even though the receiver model is steady-state, in order to minimize programming time and to generalize the model. The application of a transient solution was accomplished since the governing steady-state receiver tube equation is a first order differential equation with distance as the independent variable. The MITAS transient execution subroutine also provides the solution of a first order differential equation, however, the independent variable is time. The receiver equations were formulated so that when they were solved by MITAS as a transient problem they were actually being solved at successive distances along the tube. Formulating the problem in this mannor allows the model nodeing to be defined only at a single axial location instead of all along the length of the tube. This saves programming time and allows any length of tube to be readily analyzed. The tube length is changed by merely changing the "end time" (tube length) of the transient computer run. This approach was checked against a steady-state thermo/hydraulic problem with a known analytical solution. The comparison of the MITAS solution, using the transient execution subroutine, with the analytical solution showed that the two were essentially identical.

The thermal network for the absorber tube model is given in Figure 7. For clearity the packing is shown in a small circular region at the center of the tube while actually the packing completely fills the tube. Solar inputs are shown on the front side of the tube and on the packing. The gas is convectively coupled to the packing and to the tube front and back walls. Radiation exchange is accounted for from the packing to the tube front and back walls, to the ambient, and to the tubes' back insulation. The tube front is coupled to the ambient by both convective and radiation paths. The tube back wall is thermally connected to the ambient via a convective path to the insulation surface and then a series conduction path through the insulation to the ambient.

The features of the absorber tube model are given in Table II. Compressible flow is accounted for by treating the density of the gas as an ideal gas and by including the velocity head in the pressure drop calculations. The thermal conductivity, specific heat, and viscosity of the gas are all varied with temperature. Friction factor data from a previous test was curve fit and then used for the tube absorber analysis. This data was for a tube "lightly packed" with a steel wool type material. The equation for the friction factor is:

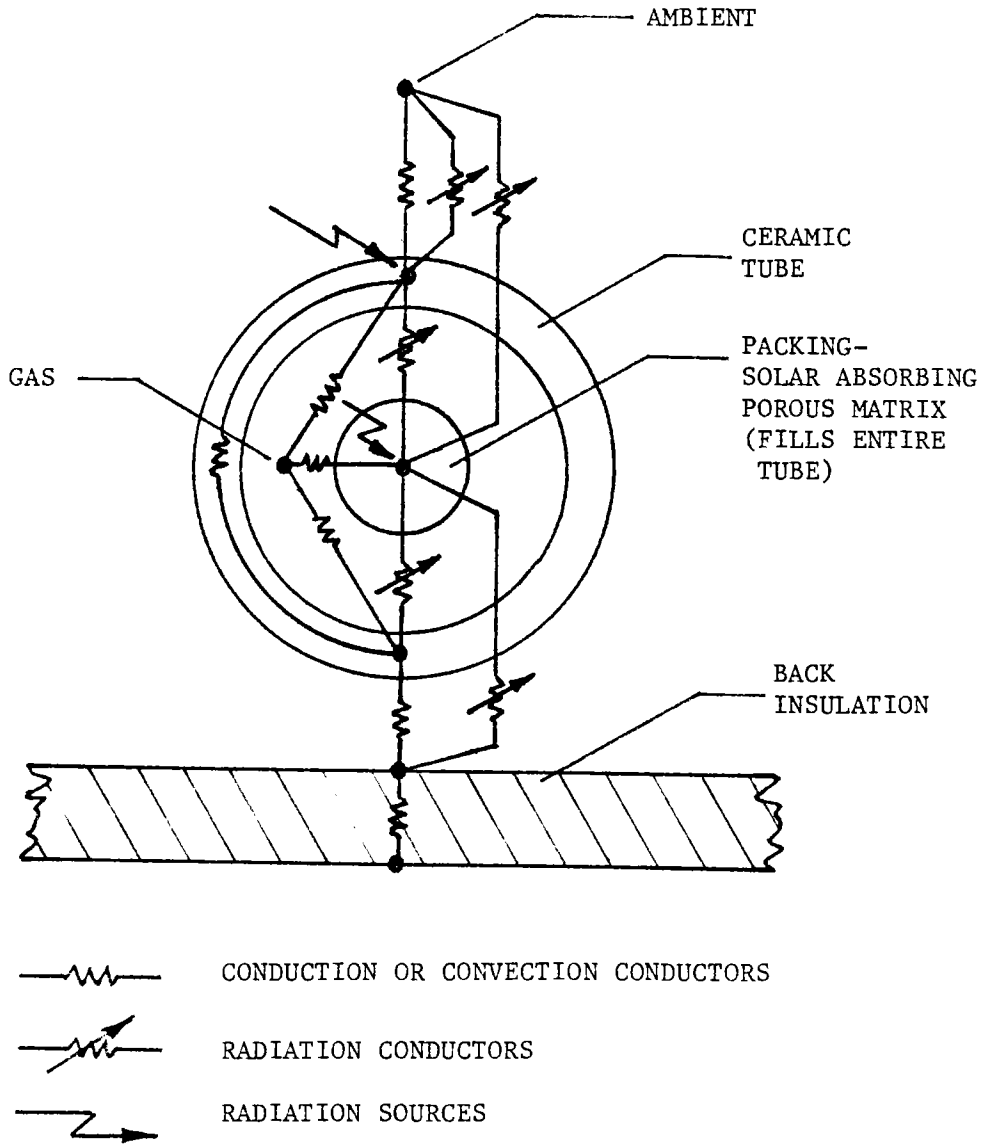

Figure 7 Receiver Tube Thermal Network

Table II Features of Absorber Tube Model

Compressible flow accounted for

Gas properties varied with temperature

Frictional pressure drop based on test data

Packing porosity automatically changed with tube diameter changes to yield optimum solar absorptance

Tube inside film coefficient based on test data

Gas to packing film coefficient based on test data

Work of compression required to offset pressure losses calculated

Program structured to minimize engineering and computer time

Convection losses based on Kraabel's correlation

(6) $f = 0.0531 + 5.12 \times 10^5/Re^{2.175}$

where,

$Re = \frac{4R_H \rho V}{\mu}$ = Reynolds number

R_H = hydraulic radius

ρ = density

V = velocity

μ = viscosity

The hydraulic radius was formulated so that as the diameter of the tube varied the solar absorbing capacity per unit area normal to the incoming flux of the packing material remained constant. This means that a small tube would absorb about the same amount of solar energy per unit area as a large diameter tube. Therefore, the porosity of the packing in a large tube would be larger for the large diameter tube than for the small diameter tube. This leads to an equation for the hydraulic radius given by:

(7) $R_H = 1.0266 \times 10^{-2} D_i - 5.364 \times 10^{-5}$, FT
Di in units of inches

The frictional pressure drop is then given by.

(8) $P_f = fL\rho v^2/R_H 2g_c$

where:

f = friction factor
L = tube length
R_H = hydraulic radius
ρ = density
V = velocity
g_c = unitary constant

The inside tube wall heat transfer film coefficient is based on experimental work reported in the technical paper. "Augmentation of Heat Transfer in Tubes by Use of Mesh and Brush Inserts," by Megertin, et al, ASME, Journal of Heat Transfer, May 1974, pp. 145 to 151. This paper stated that the ratio of augmented film coefficient to empty tube film coefficient for equal pumping power is approximately 0.7. The packing configuration used to develop this relation was a wire brush type packing. It is assumed that this configuration is appropriate for the packing which will be used for the transucent tube receiver.

The film coefficient from the packing to the gas is based on experimental work previously performed at Martin Marietta during feasibility testing of the translucent tubes. The value which was found during this testing was essentially a constant and equal to 28385 $w/(m^2-°C)$ (5000 $Btu/(hr - ft^2-°F)$).

Included in the computational package of the program is an analysis which computes the work of compression required to offset the pressure losses through the absorber tubes. The calculation is performed both for recovering the pressure loss at the inlet and at the outlet of the tubes.

The convective loss from the front (sun lite) side of the receiver tubes is based on Kraabel's correlation. This correlation is given in, "An Experimental Investigation of the Natural Convection from a Side-Facing Cubical Cavity," ASME-JSME Thermal Engineering Joint Conference Proceedings,1983, pp. 299 to 306. The area used for the convective loss calculations was one half the total tube area.

Table III shows the results of a parametric analysis of the receiver tubes. The independent quantities which were varied were the tube diameter, inlet velocity, and incident flux. The solar transmissivity, reflectivity, and absorbtivety of the tubes were taken to be 60%, 20% and 20%, respectively. These values are based of measurements taken by Martin Marietta. For all the cases shown the gas outlet temperature is essentially 1093.3°C (2000°F). Note that 50% of the reflected solar energy was assumed to be intercepted by the tubes. This was accounted for in the computations by setting the transmissivity at 70%.

Based on heliostat image size consideration, pressure drop, and temperature gradient around the tube, the 4 inch tube with the 86.75 w/cm^2 (275000 $Btu/hr-ft^2$) incident flux was chosen as the baseline. Note that the image size dictates that the absorber length can not be less than about 25 feet for a 50 MW_t receiver, or otherwise the spillage losses will become excessive.

Table IV shows the inputs to the absorber computer program while Table V shows the outputs. The output values shown are for the baseline case.

B. Receiver Configuration Design

The receiver configuration is one of the elements of the overall radiation configuration of solar thermal central receiver systems. The other principal elements of the overall radiation configuration are the height of the tower, the heliostat field layout, and the heliostat aiming strategy. The design of these interrelated elements must be integrated in order to optimize the performance of the overall system.

Table III Thermo/hydraulic Analysis - Parametric Study (SI units)

$P_i = 10^6$ Pa, T_{IN} = 538°C, T_{OUT} = 1093°C, View Factor (Tube to Aperture) = 0.25

50% of Reflected Radiation Strikes Tubes

Run	Do Cm	Di Cm	Vi m/s	Vo m/s	Q_{INC} W_2 cm	L m	ΔP Pax10^{-3}	Tube ΔT, °C	Wc/QA	QA MW	REF LOSS %	EMISS. LOSS %	CONV. LOSS %	COND. LOSS %	EFF. %
1	5.08	4.45	15.2	26.0	94.64	1.62	10.48	149.4	0.0047	.065	10	3.60	2.49	.024	83.9
2	5.08	4.45	22.9	40.1	94.64	2.41	35.37	118.9	0.0159	.098	10	3.40	2.30	.024	84.3
3	5.08	4.45	30.5	56.3	94.64	3.20	85.22	100.0	0.0378	.129	10	3.25	2.20	.024	84.5
4	7.62	6.99	15.2	26.0	94.64	2.65	10.89	153.9	0.0049	.160	10	3.70	2.51	.024	83.8
5	7.62	6.99	22.9	40.1	94.64	3.96	36.82	122.2	0.0166	.240	10	3.47	2.31	.024	84.2
6	7.62	6.99	30.5	56.6	94.64	5.27	89.63	102.2	0.0396	.320	10	3.35	2.21	.024	84.4
7	7.62	6.99	30.5	57.1	86.75	5.76	98.60	91.7	0.0435	.320	10	3.60	2.36	.026	84.0
8	7.62	6.99	30.5	57.9	78.87	6.40	109.97	80.6	0.0482	.320	10	3.91	2.54	.028	83.5
9	7.62	6.99	30.5	58.8	70.98	7.13	123.69	70.0	0.0541	.320	10	4.28	2.77	.032	82.9
10	7.62	6.99	30.5	60.1	63.09	8.11	142.10	59.4	0.0617	.320	10	4.76	3.05	.036	82.2
11	10.16	9.21	30.5	57.1	86.75	7.50	97.29	93.9	0.0429	.555	10	3.59	2.38	.026	84.0
12	10.16	9.21	30.5	57.8	78.87	8.32	108.25	82.8	0.0476	.555	10	3.90	2.56	.028	83.5
13	10.16	9.21	30.5	58.7	70.98	9.30	122.04	72.2	0.0534	.555	10	4.27	2.79	.032	82.9
14	12.7	11.75	30.5	57.9	78.87	10.82	110.32	87.2	0.0486	.903	10	3.95	2.57	.028	83.5
15	12.7	11.75	30.5	58.9	70.98	12.10	124.80	75.6	0.0546	.903	10	4.33	2.79	.032	82.8
16	12.7	11.75	30.5	60.2	63.09	13.81	144.1	64.4	0.0623	.903	10	4.81	3.07	.036	82.1

D_o = outside tube dia.

D_i = inside tube dia.

V_i = inlet velocity

V_o = outlet velocity

Q_{INC} = incident solar radiation

L = tube length

ΔP = pressure drop

Tube ΔT = front to back side tube temperature difference

W_c/QA = ratio of compressor power required to make up tube pressure drop to heat absorbed by tube

QA = heat absorbed by tube

Table III Thermo/hydraulic Analysis - Parametric Study (English units)

P_i= 145 psia, T_{IN} = 1000 ^oF, T_{OUT} = 2000^oF, View Factor (Tube to Aperture) = 0.25

50% of Reflected Radiation Strikes Tubes

Run	Do IN	Di IN	Vi FPS	Vo FPS	Q_{INC} $\frac{BTU}{HR-FT^2}$	L FT	ΔP PSI	Tube ΔT, ^oF	Wc/QA	QA MW	REF LOSS %	EMISS. LOSS %	CONV. LOSS %	COND. LOSS %	EFF. %
1	2	1.75	50	85.4	300000	5.3	1.52	269	0.0047	.065	10	3.60	2.49	.024	83.9
2	2	1.75	75	131.4	300000	7.9	5.13	214	0.0159	.098	10	3.40	2.30	.024	84.3
3	2	1.75	100	184.8	300000	10.5	12.36	180	0.0378	.129	10	3.25	2.20	.024	84.5
4	3	2.75	50	85.3	300000	8.7	1.58	277	0.0049	.160	10	3.70	2.51	.024	83.8
5	3	2.75	75	131.4	300000	13.0	5.34	220	0.0166	.240	10	3.47	2.31	.024	84.2
6	3	2.75	100	185.6	300000	17.3	13.0	184	0.0396	.320	10	3.35	2.21	.024	84.4
7	3	2.75	100	187.4	275000	18.9	14.3	165	0.0435	.320	10	3.60	2.36	.026	84.0
8	3	2.75	100	189.9	250000	21.0	16.0	145	0.0482	.320	10	3.91	2.54	.028	83.5
9	3	2.75	100	192.8	225000	23.4	17.9	126	0.0541	.320	10	4.28	2.77	.032	82.9
10	3	2.75	100	197.1	200000	26.6	20.6	107	0.0617	.320	10	4.76	3.05	.036	82.2
11	4	3.625	100	187.2	275000	24.6	14.1	169	0.0429	.555	10	3.59	2.38	.026	84.0
12	4	3.625	100	189.6	250000	27.3	15.7	149	0.0476	.555	10	3.90	2.56	.028	83.5
13	4	3.625	100	192.5	225000	30.5	17.7	130	0.0534	.555	10	4.27	2.79	.032	82.9
14	5	4.625	100	190.0	250000	35.5	16.0	157	0.0486	.903	10	3.95	2.57	.028	83.5
15	5	4.625	100	193.1	225000	39.7	18.1	136	0.0546	.903	10	4.33	2.79	.032	82.8
16	5	4.625	100	197.5	200000	45.3	20.9	116	0.0623	.903	10	4.81	3.07	.036	82.1

D_o = outside tube dia.

D_i = inside tube dia.

V_i = inlet velocity

V_o = outlet velocity

Q_{INC} = incident solar radiation

L = tube length

ΔP = pressure drop

Tube ΔT = front to back side tube temperature difference

W_c/QA = ratio of compressor power required to make up tube pressure drop to heat absorbed by tube

QA = heat absorbed by tube

Table IV Absorber Tube Computer Program Inputs

```
TSTEPI = 0.05 $LENGTH OF NODE, FT
1  = 4.0      $OUTSIDE TUBE DIA, INCHES
2  = 3.625    $INSIDE TUBE DIA, INCHES
3  = 0.8      $COMPRESSOR EFFICIENCY
4  = 2000.    $MAXIMUM GAS TEMPERATURE, F
5  = 12.0     $BACK INSUL THICKNESS, INCHES
6  = 275000.  $INCIDENT FLUX, BTU/HR FTSQ
7  = 1000.    $INLET TEMPERATURE, F
8  = 145.     $INLET PRESSURE, PSIA
9  = 100.0    $INLET VELOCITY, FPS
10 = 100.     $AMBIENT TEMPERATURE, F
11 = 14.7     $AMBIENT PRESSURE, PSIA
12 = 0.7      $SOLAR TRANSMISSIVITY OF TUBE
13 = 0.2      $SOLAR EMISSIVITY OF TUBE
14 = 0.6      $IR TRANSMISSIVITY OF TUBE
15 = 0.2      $IR EMISSIVITY OF TUBE
16 = 0.25     $VIEW FACTOR--TUBE TO APERTURE
17 = 1.0      $CORR. FACTOR--TUBE EXTERIOR TO AMBIENT
18 = 1.0      $CORR. FACTOR--PACKING FILM COEF
19 = 0.05     $CONDUCTIVITY OF BACK INSULATION, BTU/HR-FT-F
20 = 55.15    $GAS CONSTANT, FT-LBF/LBM-F
21 = 0.7      $CORR. FACTOR-- TUBE INTERIOR FILM COEF.
```

Table V Absorber Tube Computer Program Outputs

```
------------------------------------------------
------------------DIMENSIONS--------------------
TUBE O.D. =  4.00 IN.   TUBE I.D. =  3.625 IN.
DISTANCE FROM INLET=  24.60 FT
--------------INLET CONDITIONS--------------------
      GAS TEMP. = 1000.0 F
      GAS PRESSURE=  145.0 PSIA
      GAS VELOCITY=  100.0 FT/SEC
      MASS RATE OF FLOW=     6689.11 LB/HR
      INCIDENT FLUX=   275000.0 BTU/HR-FTSQ
----------EXIT CONDITIONS (ACTUAL)-----------------
      GAS TEMP. =  2001.1817 F
      TUBE FRONT TEMP. =  2183.6547 F
      TUBE BACK TEMP. =  2014.5455 F
      PACKING TEMP. =  2007.5849 F
      GAS PRESSURE=  130.51609 PSIA
      GAS VELOCITY=  187.23437 FT/SEC
      MACH NO. =    .0780
      REYNOLDS NO. =  2.4107E+05(DIA)    1.1862E+05(HYD. RADIUS)
      RATIO OF ACTUAL TO EMPTY TUBE PRESSURE DROP=      34.358
-EXIT CONDITIONS WITH VEL REDUCED TO INLET VALUE-
      TEMP. =  2002.8881 F
      PRESSURE=  130.89061 PSIA
      EXIT TUBE DIA. =   4.95 INCHES
---GAS EXIT PRESSURIZED TO INLET PRESSURE------
      TEMP. =  2080.0676 F
      WORK OF COMPRESSION=      1.51E+05 BTU/HR
      COMPRESSOR EFFICIENCY=    .80
      RATIO OF WORK TO HEAT ABSORBED=      7.98E-02
---------------ENERGY FLUXES--------------------
      INCIDENT=   2255000.0 BTU/HR
      REFLECTION=    225500.0 BTU/HR---   10.000 PERCENT
      EMISSION  =     80323.6 BTU/HR---    3.562 PERCENT
      CONVECTION=     52915.3 BTU/HR---    2.347 PERCENT
      CONDUCTION=       582.8 BTU/HR---     .026 PERCENT
      ABSORBED  =   1895656.2 BTU/HR---   84.065 PERCENT
---WORK REQUIRED TO RECOVER PRESSURE LOSS---
      COMP. WORK (INLET CONDITIONS)=      81349.1525 BTU/HR
      COMPRESSOR EFFICIENCY=    .80
      RATIO -WORK OF COMP. TO HEAT ABS=    4.291E-02
```

A major concern relative to the design of high temperature gas receivers is the potentially large infrared and convection losses associated with the high operating temperatures. In order to minimize these losses, it is imperative that a cavity type receiver be used for this application with special provisions made to minimize the aperature area and to enhance hot air stratification inside the cavity. An approach for minimizing the aperature size is to use high quality heliostats, with near-perfect focusing, in strategic locations in the heliostat field. These high quality heliostats would have a focal length equal to the slant range and would be able to direct the reflected central beams of all the mirror elements of each heliostat through a common aim point. Also, the effective beam divergence angle (EBDA) of the high quality heliostats will be smaller than the 50 to 60 minutes of arc which is used for commercial quality heliostats.

Note that the ideal EBDA for a perfect heliostat is 32.2 minutes of arc, the angular size of the solar disk, and heliostats have been tested at the Central Receiver Test Facility which have an EBDA of 40 minutes of arc. It is assumed that the high quality heliostats will exhibit an EBDA of 40 minutes of arc.

The heliostat field layout for the 50 MW_t system is shown in Figure 8. The optimum height of the tower associated with this field is 83 m (272.3 ft). If the entire field consisted of commercial - quality heliostats with EBDA'S of 50 minutes of arc, the theoretical image size in the aperture plane would be 9 m (29.5 ft) in diameter. However, if high quality heliostats with an EBDA of 40 minutes of arc are used in the area between the two excentric circles on Figure 8, the image size at the plane of the aperture is reduced to 7 m (23 ft). We recommend this approach along with the receiver design shown on Figure 9.

The proposed receiver design has a cavity depth of 6.1 m (20ft). If single point heliostat aiming is used, the peak solar flux on the absorber would be 95 watts/cm^2 (301,000 Btu/hr-ft^2) with an insolation of 0.09 watts/cm^2 (285.3 Btu/hr-ft^2). By using an aiming strategy comprised of six aiming zones the solar fluxes can be flattened as shown on Figure 10. This provides a 25% margin in maximum solar fluxes relative to the 86.75 watts/cm^2 (275,000 Btu/hr. ft^2) value consistent with the baseline identified in the thermo/hydraulic optimization.

It is interesting to note at this point that the translucent tubes exhibit the ability to absorb very high solar fluxes. Therefore, it appears that translucent tube gas receiver sizes may be dominated by heliostat image size considerations rather than flux level constraints on the absorber surface.

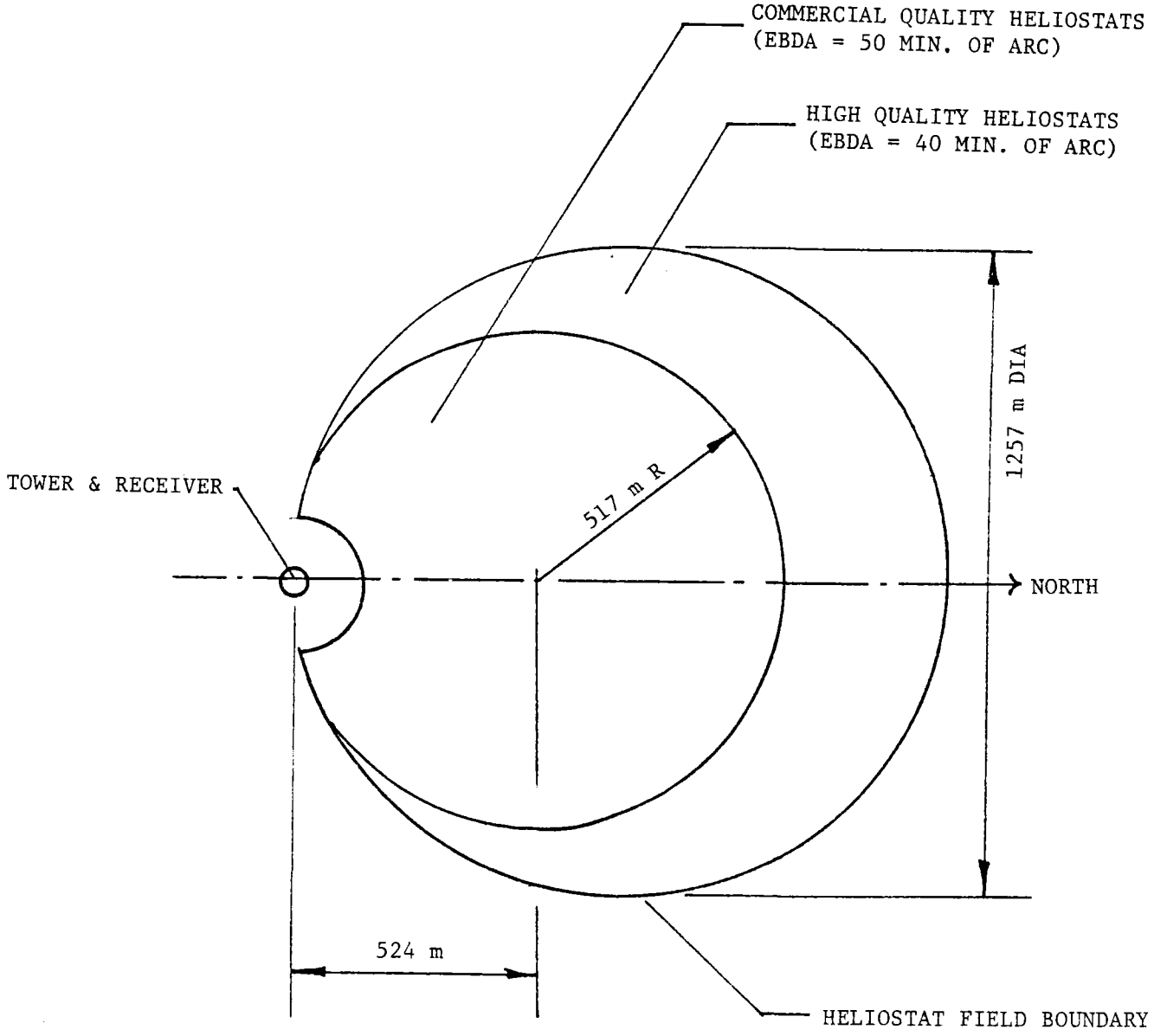

Figure 8 Heliostat Field Layout

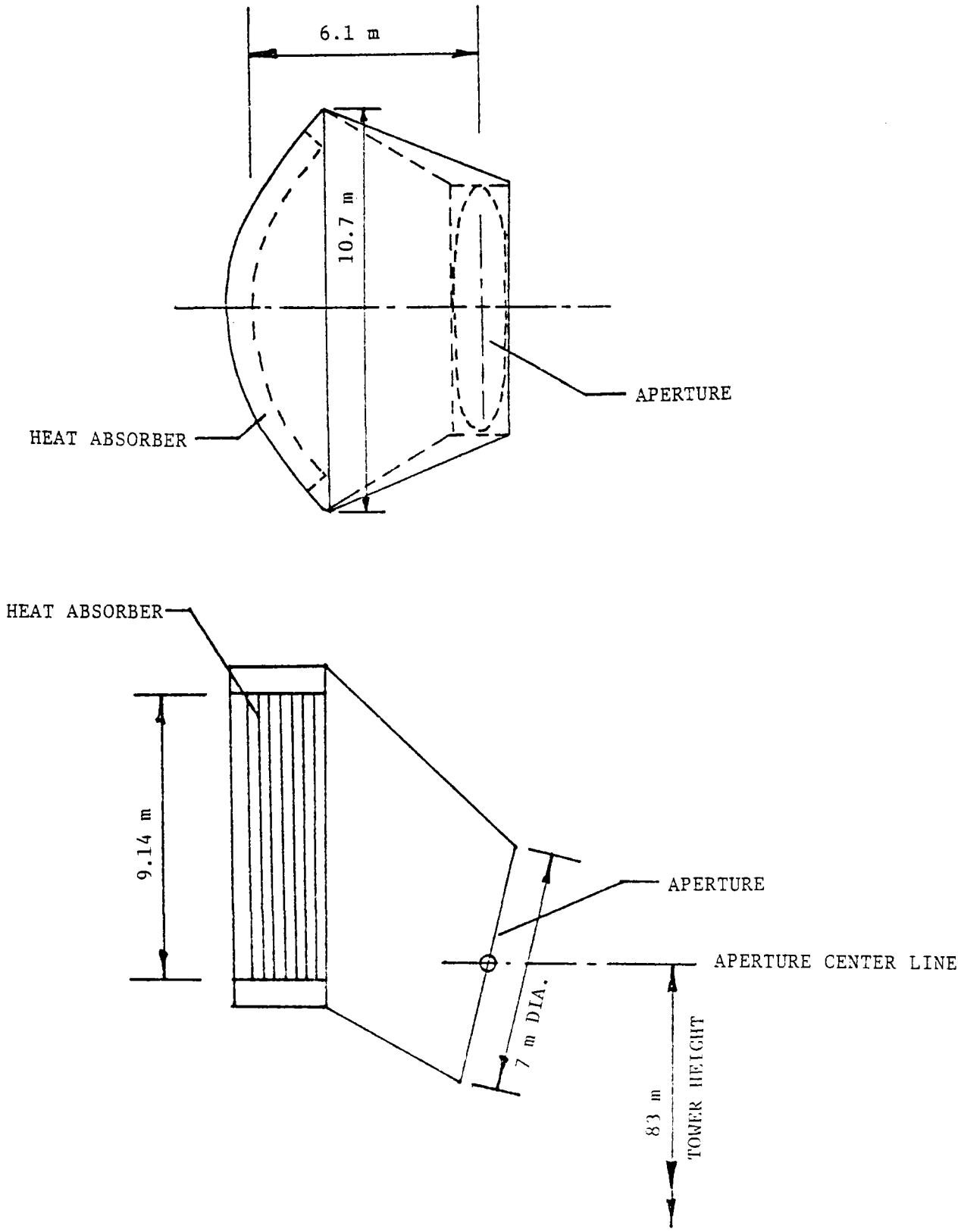

Figure 9 Commercial Scale Receiver Cavity Design

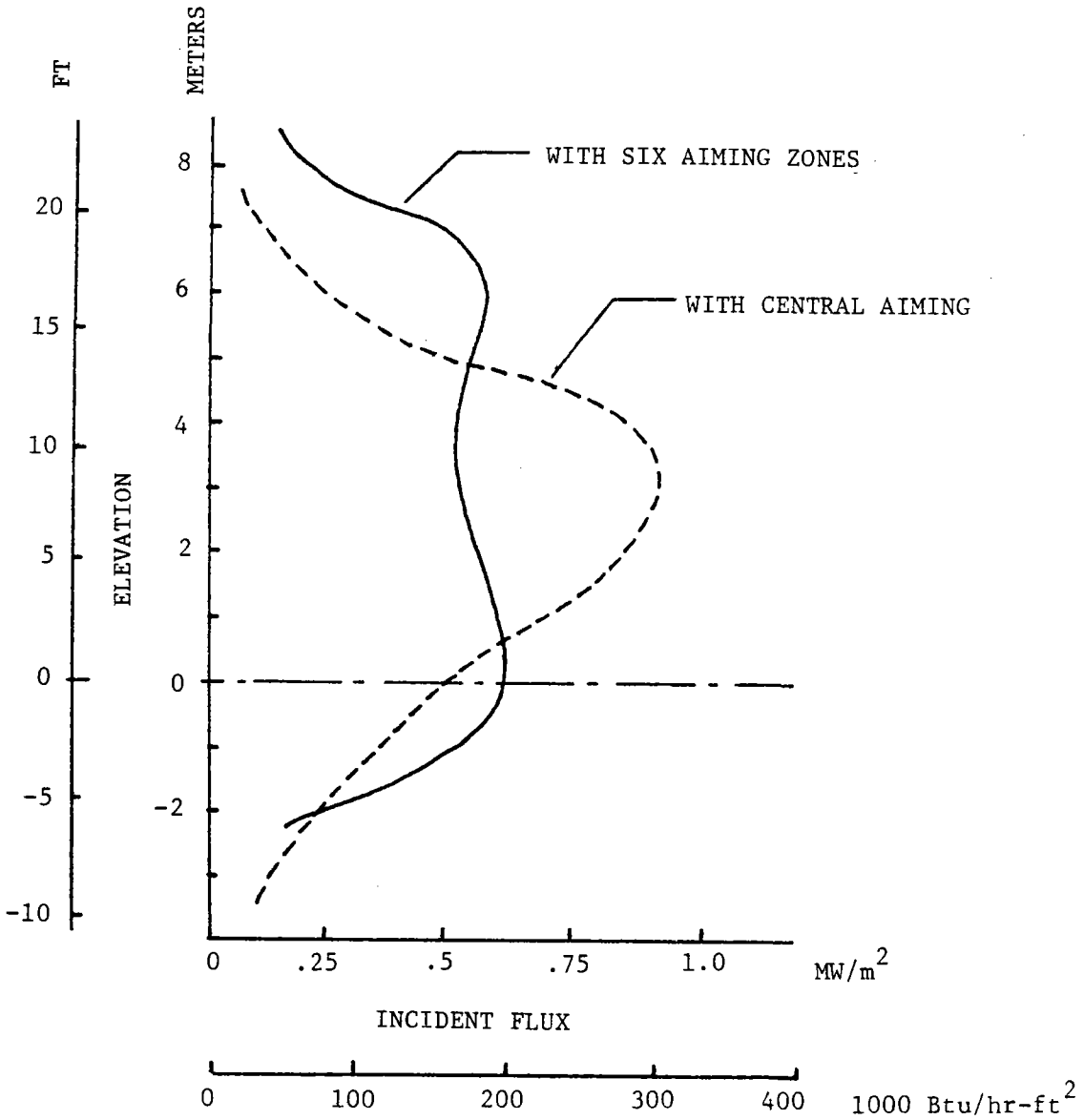

Figure 10 Flux Distribution on Center Tube

C. Design Details

The properties of the alpha-alumina tube material are given in Table VI. A curve of transverse strength vs. temperature is given in Figure 11 and a curve showing the fatigue strength of the material is given in Figure 12. Data from Figures 11 and 12 are used to estimate the allowable strength (transverse) for the alpha-alumina in solar receiver service. For a maximum outlet gas temperature of 1093.3°C (2000F) it is assumed that the corresponding maximum tube temperature is approximately 1149°C (2100°F). From the curve on Figure 11 the ratio of the strength at 1149°C (2100°F) to the strength at room temperature is 17800/30700 = 0.58. In regard to fatigue, it is assumed a commercial receiver will cycle from low to high temperatures, and thus produce a stress cycle, once each clear day and an average of ten times each partly cloudy day. The cycles on a partly cloudy day are due to cloud transients. On cloudy days it is assumed the receiver is not brought on line and, therefore, there are no cycles. The total number of cycles for a commercial receiver are estimated based on the solar conditions at the Central Receiver Test Facility in Albuquerque, New Mexico. At this location there are an average of 174 clear days, 108 partly cloudy days, and 83 cloudy days per year. If the design life of the commercial receiver is 30 years then the total number of cycles are (174 + 108 x 10) x 30 = 37,620. Using this value along with the fatigue curve on Figure 12, the reduction in strength due to fatigue is 23500/36400 = 0.65. If it is assumed that the temperature and fatigue effects can be linearily combined the resulting maximum working stress for the receiver tubes is:

Maximum working stress = 39900x 0.58 x 0.65
= 15000 psi
= 1.034×10^8 Pa

The curve given in Figure 13 provides data relative to the thermal shock resistance of alumina. The curve shows the maximum initial temperature prior to quenching for a sheet of alumina. At temperatures higher than those shown the alumina will fail on quenching. The maximum temperatures are given as a function of the parameter a·h. The quantity "a" is the thickness of the sheet in feet and "h" is the film coefficient in units of Btu/hr-ft^2°F. For a sheet thickness of 1/4 inch and a typical free convection film coefficient of 2.0 Btu/hr-ft^2°F, the numerical value of a·h is 0.042. This value corresponds to an initial temperature of over 538°C (1000°F) which is safe for quenching in ambient air.

The strength, fatigue, and thermal shock data given in this report were taken from, "Mechanical Properties of Engineering Ceramics," Interscience Publishers, New York, 1961. The thermal shock data is from page 153, the strength data from page 155, and the fatigue data from page 290.

Table VI Aluminum Oxide Properties

(properties are at room temperature unless otherwise stated)

Microstructure	Polycrystalline
Crystalline Phase	Alpha Alumina
Purity	99.9% Al_2O_3
Average Grain Size	30 microns
Melting Point	2040°C (3704°F)
Specific Gravity	3.97
Modulus of Rupture	2.75×10^8 Pa (3.99×10^4 psi)
Compressive Strength	2.24×10^9 Pa (3.25×10^5 psi)
Young's Modulus	3.93×10^{14} Pa (5.7×10^7 psi)
Poisson's Ratio	0.23
Solar Absorptivity	0.2
Solar Reflectivity	0.2
Solar Transmissivity	0.6
Thermal Conductivity	
at 126.6°C (260°F)	- 2.92 w/cm-°C (169 BTU/HR-FT-°F)
at 1226.7°C (2240°F)	- 0.62 w/cm-°C (36 BTU/HR-FT-°F)
Specific Heat	0.21 cal/gm-°C (0.21 BTU/LB-°F)

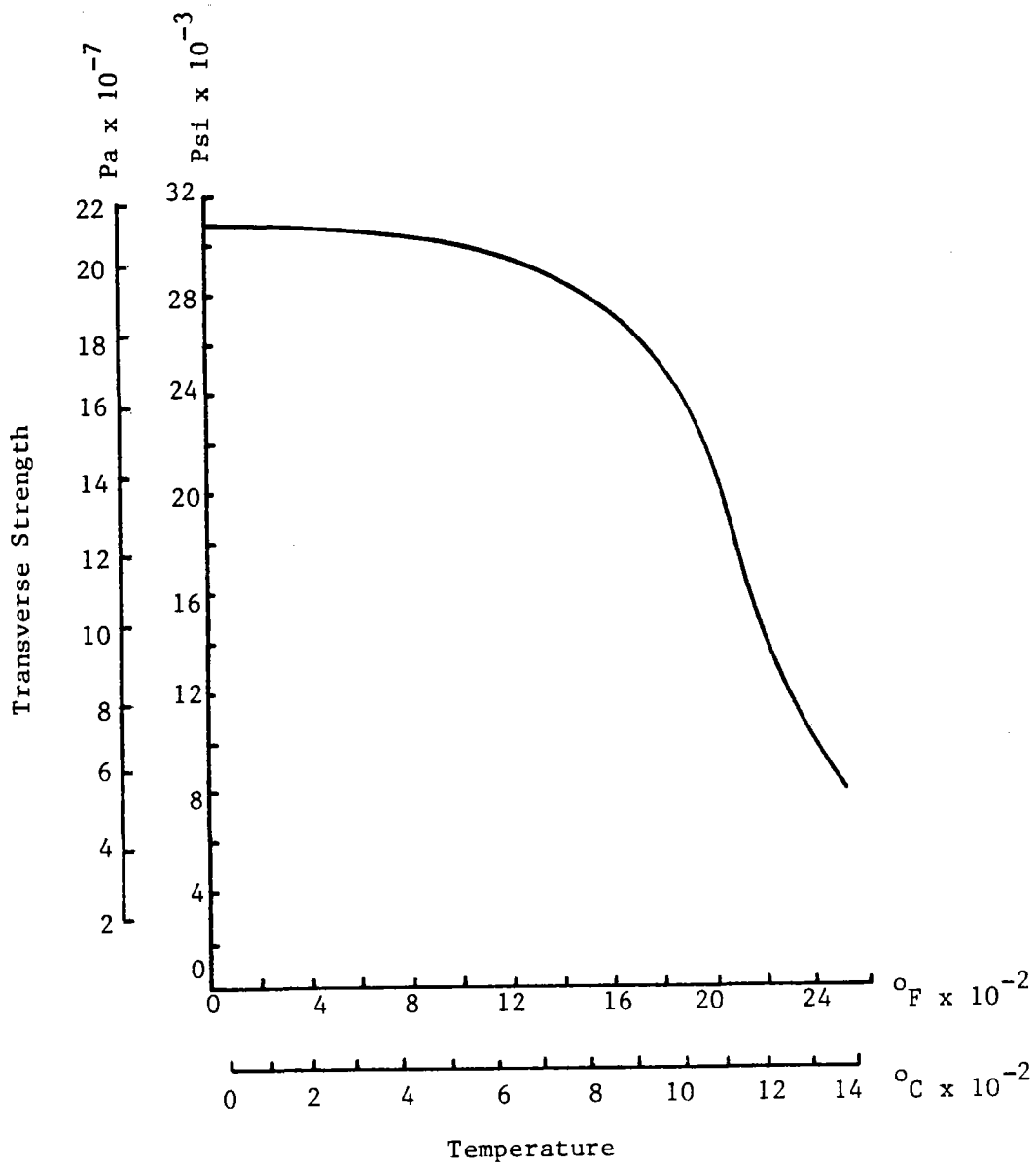

Figure 11 Transverse Strength of Alumina vs Temperature

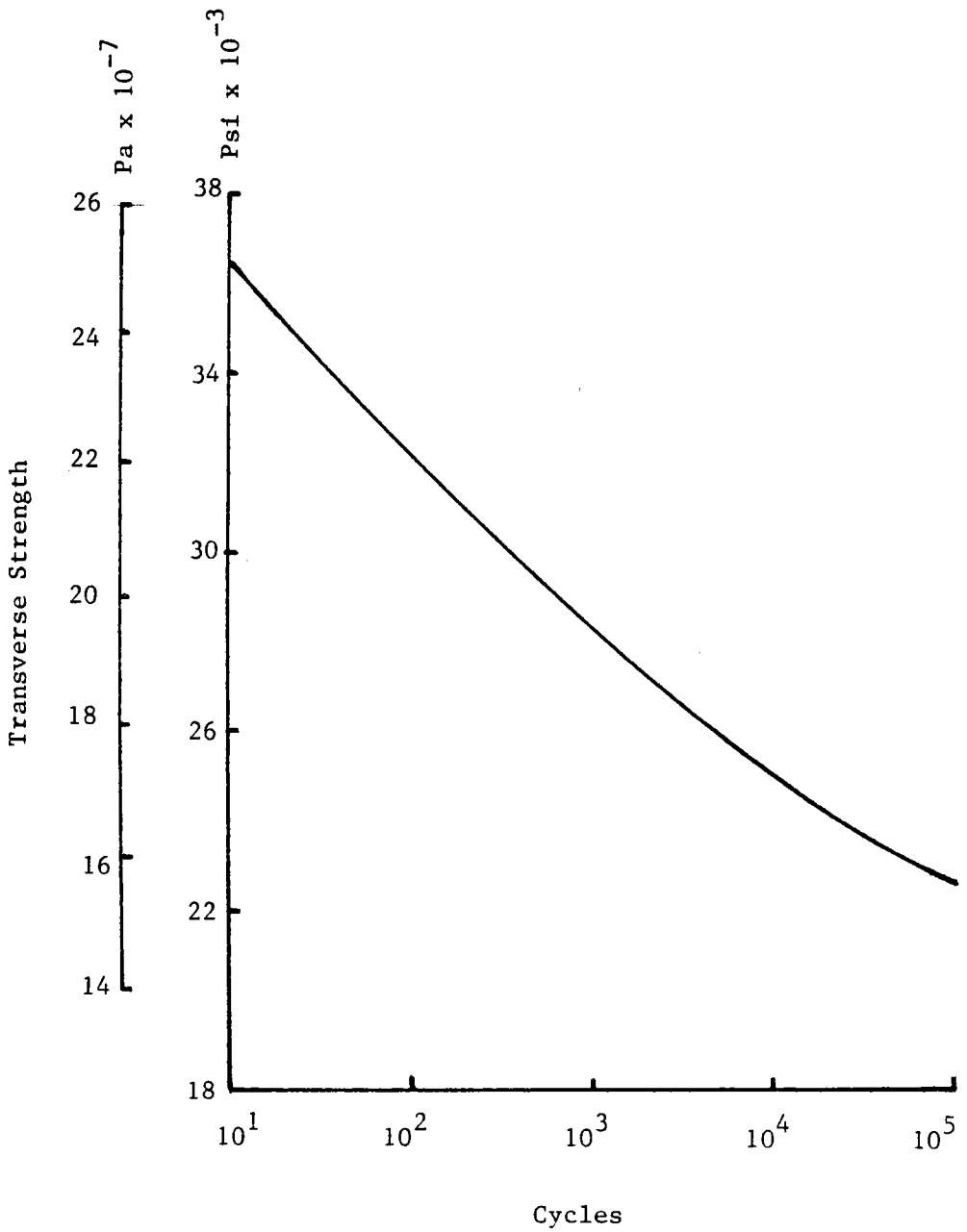

Figure 12 Fatigue Curve for Alumina

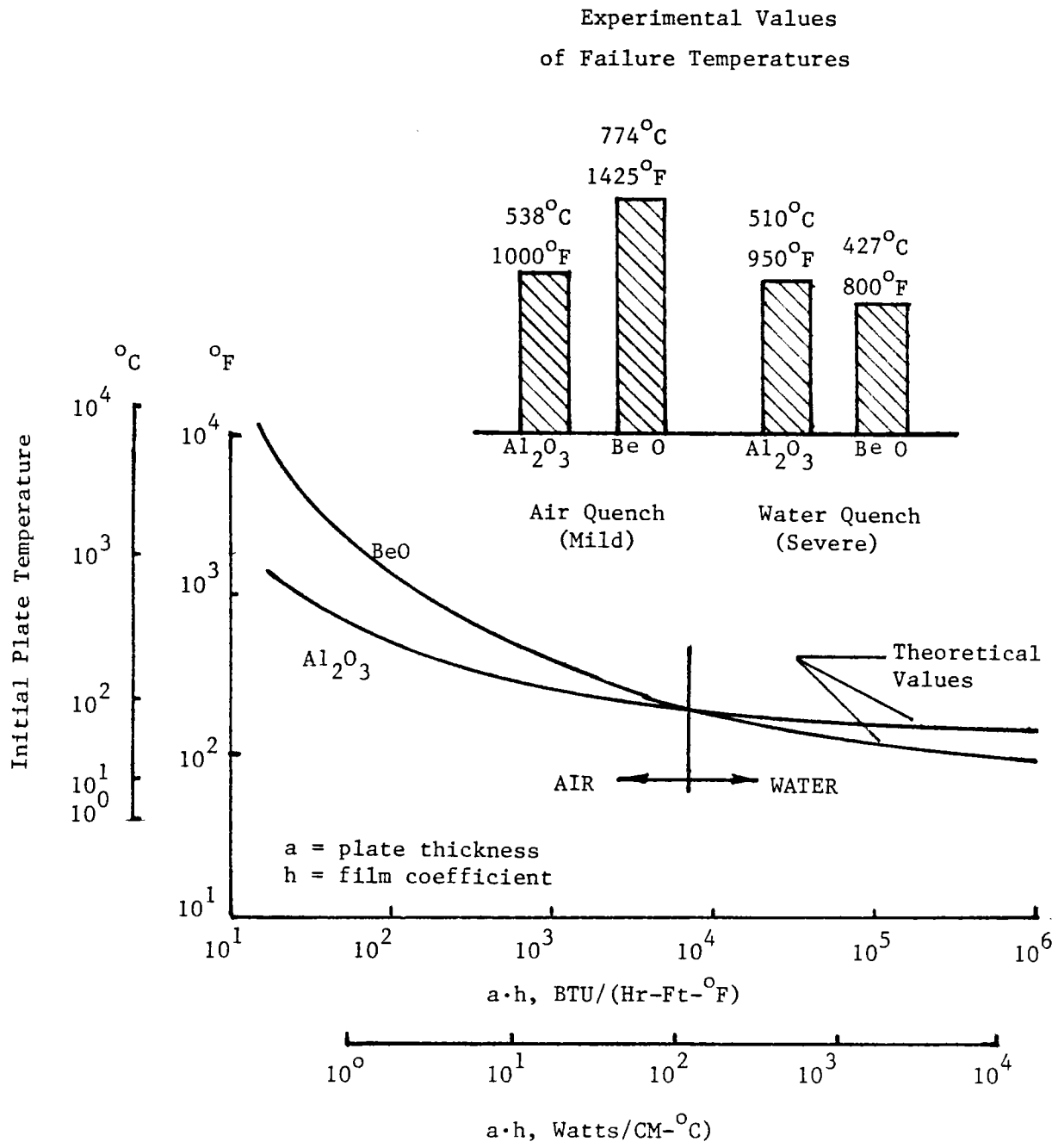

Figure 13 Experimental and Theoretical Thermal Shock Data

Thermal shock tests were performed during this contract using solar energy as the heating source. These solar shock tests showed that the alpha-alumina is appropriate for solar receiver operation and that thermal shocking from the heliostats should not be a problem. These tests are described in detail in Section IV of this report.

Thermal stresses are induced in the receiver tubes since the incoming solar flux is directional and strikes the tubes generally over the tube surface facing the heliostat field. This uneven heating of the tubes give rise to circumferential temperature gradients which, in term, cause thermally induced stresses. These stress levels were estimated using the equation given in the report, "Alternate Central Receiver Power System, Phase II," Volume II, May 1981, p. IV-64.

$$S = \frac{(T_f - T_b)}{4} \alpha E$$

where,

S = stress
T_f = tube front side temperature
T_b = tube back side temperature
α = coefficient of thermal expansion
E = Young's Modules

Using this equation and an allowable stress of 1.034×10^8Pa (15000 psi) the allowable temperature difference ($T_f - T_b$) can be evaluated. This temperature difference is plotted vs the gas temperature (assumed to be equal to the tube back temperature) and shown on Figure 14. The variation of the allowable temperature difference with gas temperature is due to the temperature dependence of the coefficient of thermal expansion. At 1093°C (2000°F) the maximum difference is approximately 133°C (240°F). Applying a 20% margin yields a maximum temperature difference of 111° (200°F) which is the value used for the receiver tube thermo/hydraulic evaluation.

It is interesting to note that a receiver tube with an average temperature difference of 200°F from front to back will deflect about 6.6 cm (2.6 inches). This is the case asssuming the tube diameter is 10.2 cm (4 inches) and the length is 7.62m (25 ft).

Ceep does not appear to be a problem for the alumina in receiver applications. Creep data were found for the alumina at 1000°C (1832°F) in "Mechanical Properties of Engineering Ceramics," by Kriegel and Palmour, Interscience, 1961, page 305. These data were curve fit to yield the equation,

$S = 0.25 (T_F - T_B)\alpha E$ = thermal stress

$\alpha = a + b (T_F + T_B)/2$

α = Coef. of thermal expansion

E = Young's Modulus

T_F = Front Side Temp

T_B = Back Side Temp

Tgas = Gas Temp

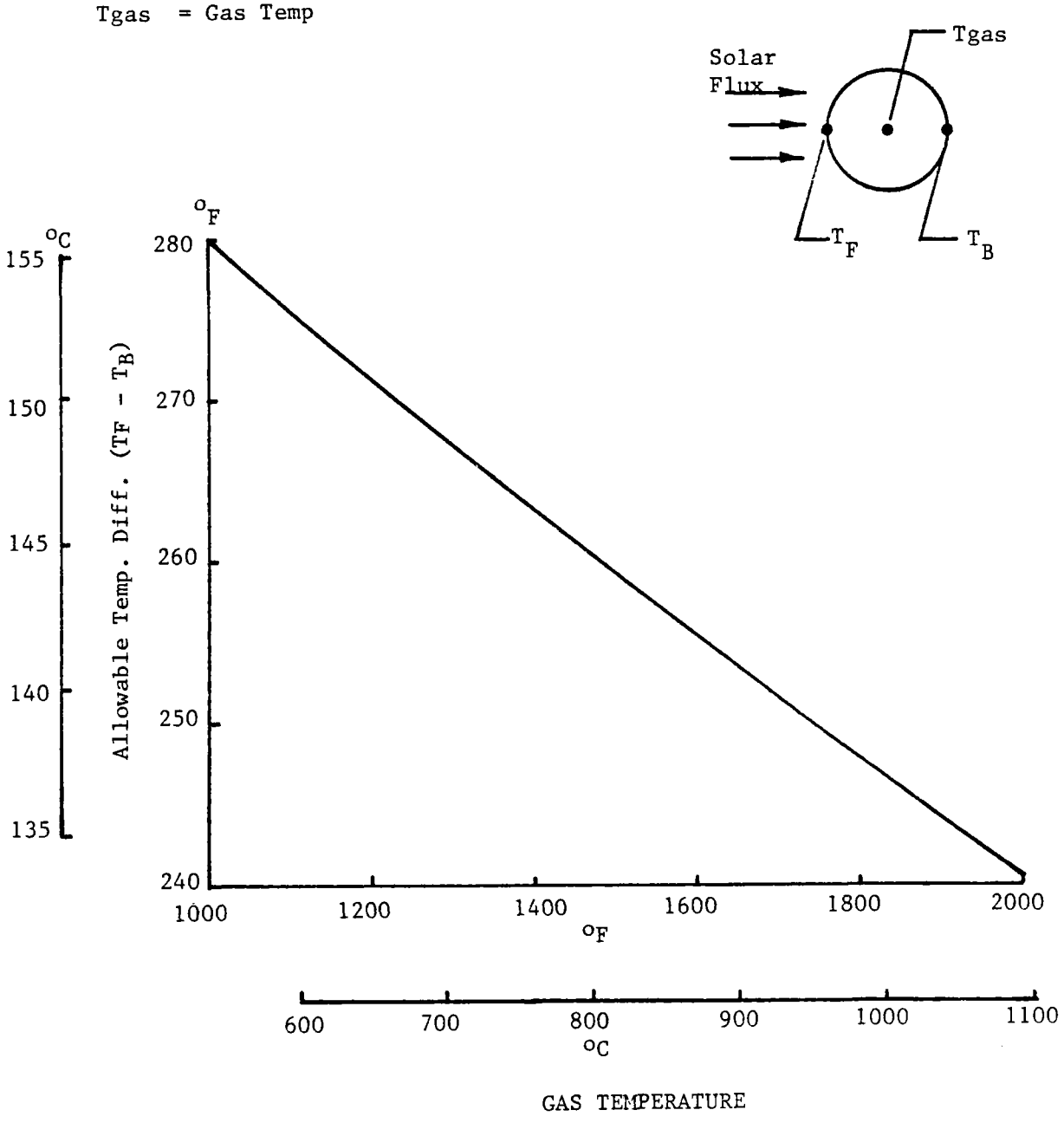

Figure 14 Allowable Front to Back Temperature Difference Vs Gas Temperature with Regard to Thermal Stress

$$(10)\quad C_R = 2.5L^{5.9}$$

Where,

C_R = creep rate in microus/hour
L = load in kg for a simply supported rod 3 inches long and 0.1 inches in diameter

Equation (10) can be re-arranged, using standard beam relationships to the form,

$$(11)\quad C_r = 2.94 \times 10^{-25} S^{5.9}$$

where,

C_R = creep rate in microus/hour
S = stress in psi

If the stress which would result from an internal pressure of 10^6Pa (145 psi), the assumed working pressure of the receiver, is substituted into equation (11), the resulting creep rate would only cause an elongation of 0.00005 cm (0.00002 inches) in 30 years. This amount of creep is certainly of no concern.

The baseline tube attachment/coupling scheme is shown in Figure 4. The lower attachment/coupling is similar to the design proposed by Black and Veatch for their opaque ceramic tube receiver. This approach has been analyzed and tested by AiResearch under the EPRI contract, "Analysis of Thermal and Mechanical Stresses in the Ceramic Seal of the 1-MW(th) Bench - Model Solar Receiver" (AP-2267, Research Project 475-9). The upper attachment/coupling is a one-stage labyrinth type seal which allows unconstrained thermal growth along the axis of the tube. Also with an initial 0.0102 cm (0.004 inches) gap clearance, it is unlikely that thermal distortions will cause interference between the tube and the seal. For example, suppose the steel supports which support the inlet and the outlet of the vertical receiver tube are effected by the inlet and outlet temperature over a two foot horizontal lengths. Also, assume these steel supports will have a difference in average temperature of 555.5°C (1000°F). This temperature difference in the inlet and outlet tube supports would cause an offset of 0.61 cm (0.24 inches) between the center line of the tube outlet and tube inlet relative to the vertical. If this is arbitrarily increased by 50% the resulting angle between the tube and the vertical would be 0.0614 degrees. With this angle, θ , fixed it is possible to establish a relationship between β, the angle between the plane of the seal and the horizontal and the thickness of the seal, Z. A sketch defining the seal clearance parameters is shown on Figure 15. The analysis of the clearances which relates the allowable angle β relative to

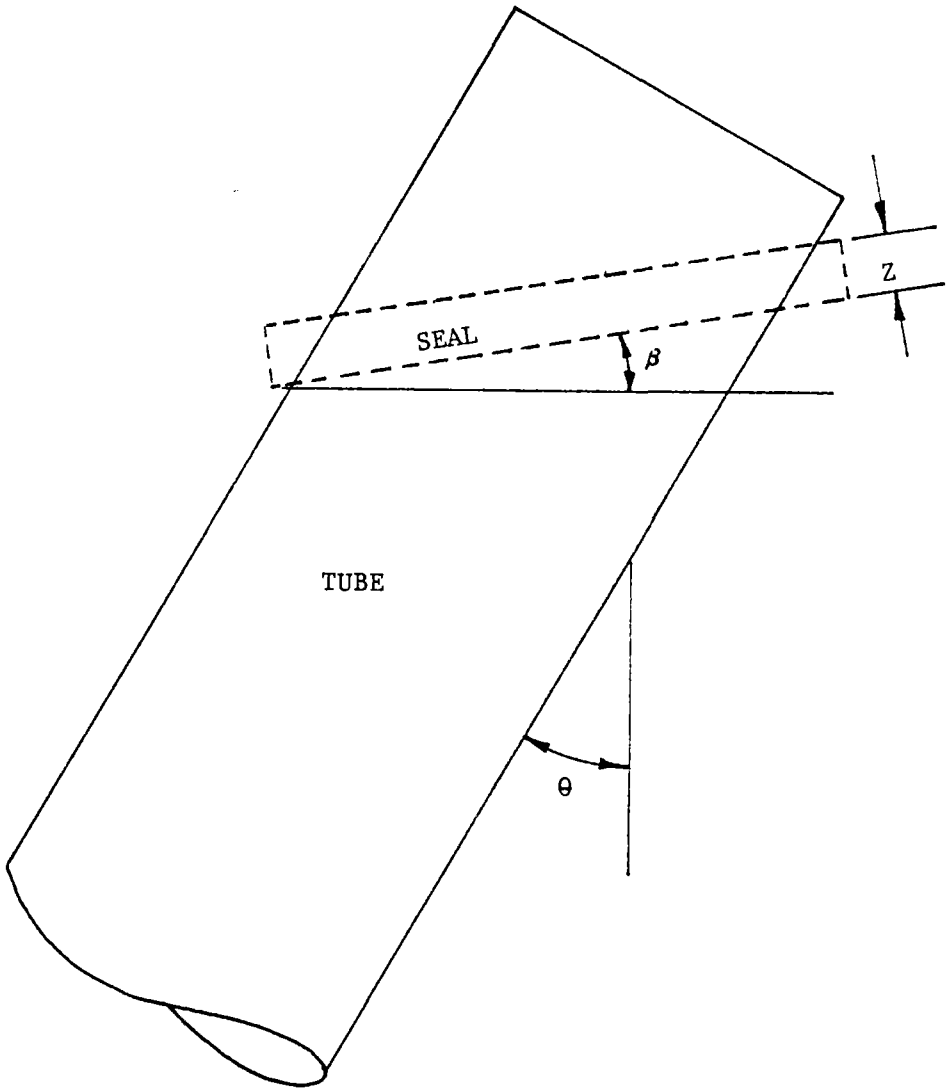

For θ = 0.0614^{o}

β, Deg	Z	
	CM	IN
2.1	0.318	0.125
2.7	0.159	0.0625
3.3	0.0254	0.01

Figure 15 Labyrinth Seal Clearance

the seal thickness, Z, is also shown on the figure. It is interesting to note that if the angle β, between the plane of the seal and the horizontal, is 3.3° this would correspond to a rise of 3.51 cm (1.38 inches) over a 0.61 m (2 ft) run. It certainly seems unlikely that a distortion of this magnitude would occur due to either alignment problems or thermally induced distortions or a combination of the two.

The mechanical characteristics of the tube configuration shown in Figure 4 are discussed in this paragraph. The thermal growth of the tube in the axial direction is 5.8cm (2.28 inches). This presents no problem since the design allows vertually unlimited growth in this direction. Radial thermal growth at the inlet (cold) end of the tubes is 0.042 cm (0.0167 inches) but this is compensated by the growth of the seal which is made of the same material as the tube, alpha-alumina. Radial thermal growth of the tube at the outlet is 0.0996cm (0.0392 inches), however, the design of the outlet attachment/coupling can easily accommodate this growth. The pressure assumed for the baseline system is 10^6 Pa (145 psia). This pressure level causes a stress of 9.156×10^5 Pa (1328 psi) in the baseline tube which has an outside diameter of 10.2cm (4 inches) and a wall thickness of 0.476cm (0.1875 inches). Using the allowable flexture stress of 1.034×10^8 Pa (15000 psi), which includes allowances for both temperature and fatigue, the safety factor is 11.3. This safety factor is based on the flexture strength of the tube material. Relative to compressive loads the safety factor of the material is on the order of 1000. With regard to wind loads and assuming a safety factor of two, the tubes can be subjected to a wind of 4.6 m/s (10.3 mph) without being over stressed. Inside a cavity the tubes should never experience a 4.6 m/s (10.3 mph) wind especially since the cavity doors are closed when the wind speed is about 15.6 m/s (35 mph). The cavity doors are always closed when this condition exists since the heliostats can not operate at wind speeds at or above 15.6 m/s (35 mph). Finally, it was established that the receiver tubes can experience a horizontal g loading of 5.7 before failure. The acceptable g loading in the vertical would be many times the 5.7 value. Earthquakes which cause a g loading of 5.7 are very uncommon.

A feature of the proposed design which may be practical is the spinning of the tubes about their vertical axes. This could be accomplished by inserting a vane or blades within the tubes and powering the rotation with the gas which flows through the tubes. The power

required to rotate a tube at 60 RPM is estimated to be about 1.94×10^{-4} MW which is only 0.035% of the power absorbed by the gas flowing through the tube. The purpose of spinning the tubes is to decrease the temperature gradients around the tubes and thereby reduce or eliminate thermal stresses. A secondary benefit would be that the spinning will increase the gas film coefficients and therefore improve the thermal performance of the tubes. At 60 RPM the temperature differences at any axial location on the spinning tubes will be approximately 0.55° (1°F). If the tubes are stationary the temperature difference could be 93.9 °C (169°F) from front to back of the tubes.

The equation which was derived to estimate the temperature differences, front to back of the tubes, is as follows,

$$(12)\quad T = T_a\,(1 - e^{-\alpha\tau}) + T(0)\,e^{-\alpha\tau} + \beta\gamma\left[\frac{e^{-\alpha\tau}}{\alpha^2+\beta^2} + \frac{\sin(\beta\tau - \tan^{-1}\beta/\alpha)}{\beta(\alpha^2+\beta^2)^{1/2}}\right]$$

where,

L	=	$h/\delta\,\rho\,C_p$, $\beta = 2\pi R$, $\gamma = q/\delta\rho Cp$
h	=	tube to ambient film coefficient
δ	=	thickness of tube wall
ρ	=	density of tube material
C_p	=	specific heat of tube material
R	=	rotational speed of tube, RPM
q	=	solar energy absorbed per unit area
T_a	=	ambient temperature
T	=	tube temperature
$T(0)$	=	initial tube temperature as tube rotates into sun
τ	=	time

The tube temperature, T, defined in equation (12) is the temperature at a point on the rotating tube. This point rotates with the tube and moves in and out of the sun. The temperature, T(0), is defined as the temperature of a point at the time the point has just emerged into the sunlight. It is assumed that the incident solar flux is columnated, therefore, the point is irradiated during one half revolution and is in the shade during the other half. Since the shady side of the tube is insulated it is assumed that the tube temperature is constant while in the shade. Therefore, the temperature of a point just emerging into the sun, T(0), equals the temperature of the point as it just rotates into the

shade. Equation (12) was solved by meeting this condition for given values of h, q, and R. The front to back temperature difference was found, then, by computing the maximum sun lite side temperature and subtracting the shady side temperature, T(0). The results of this calculation are given below.

RPM	Front to back temperature difference	
	°C	°F
1	43.6	78.4
10	3.7	6.6
60	0.61	1.1

IV MATERIALS INVESTIGATIONS

Thermal shock tests were conducted on the alpha-alumina tube material by the Advanced Components Test Facility at the Georgia Institute of Technology. These tests consisted of subjecting 0.86 cm (0.34 inch) outside diameter alpha-alumina tube samples to step solar inputs of approximately 60 watts/cm^2 (190300 Btu/hr-ft^2) and 100 watts/cm^2 (317000 Btu/hr-ft^2). The tubes survived the thermal shock at the lower input condition but failed at the higher flux level. The failure is thought to have occurred due to a dark spot on the tube which was a result of the melting of the insulation of a thermocouple which was positioned on the inside of the tube. This failure is no cause for concern, however, since an operational solar receiver would never have step changes in the incident solar radiation of even a small fraction of the levels used in the Georgia Tech tests.

The tubes which were irradiated during the thermal shock tests did experience a color change (darkening) during the short exposure time used for the thermal shock tests. One possible explanation for the change was that outgasing from adjacent thermal insulation could have deposited on the tube surface. This possibility was discussed with Georgia Tech personnel. Their feeling was that the outgasing was a remote possibility since the cavity used to hold the specimen had been operated for several hours at high temperatures prior to the ceramic tube tests. This suggests that any materials which are prone to outgas would have long since been depleted of any source for outgasing.

This conclusion is supported by careful inspection of the discolored tubes. The inspection included an attempt to sand the surface of the tubes and the breaking of the tubes so that a cross section could be inspected. Sanding the tube surface did not reveal any kind of surface coating and the inspection of the cross section of the broken tube appeared to show a discoloration throughout the tube material.

The discoloration of the alpha-alumina material apparently is due to either the solar flux, the temperature, or a combination of high solar flux and temperature. In 1981 tests were performed by Martin Marietta to establish the radiation characteristics of the alpha-alumina material. These tests were conducted under Independent Research and Development (IRAD) funding and included the temperature effects on the transmissivity of alpha-alumina. These tests showed that the transmissivity of the alpha-alumina was essentially equal before and after being heated to 816°C (1500°F) for four weeks in an electric furnace. The material used in this test was from the same vendor, GE, as the tube material used in the Georgia Tech tests. The results of our IRAD tests suggests that the cause of the discoloration was the solar flux.

A potential problem which is as serious as the discoloration is the availability of the alpha-alumina material in tube sizes appropriate for the absorber tubes of a commercial size central receiver. The size which appears optimum for a $50MW_t$ central receiver is about 10.2 cm (4 inches) in diameter and 8.5 m (28 ft) long. We have contacted General Electric, Coors Porcelain, and Ceramatic in regard to obtaining tubes of this size. All of these companies reported that not only is this length tubing unavailable at this time but that it does not appear economically feasible to produce tube more than about 1 m long in the forseeable future. Tubes of 10.2 cm (4 inches) in diameter, and larger, and 1 meter in length are currently available.

V. CONCLUSIONS AND RECOMMENDATIONS

There are two significant potential problems which have been identified relative to the use of alpha-alumina for solar thermal central receiver applications. These are the discoloration of the material when subjected to high solar fluxes and the unavailability of the material in tubing lengths on the order of about 8.5 m (28 ft). This is the length which is appropriate for receivers with a 50 MW_t rating. The 50 MW_t rating is about the minimum size commercial plant that would be economically feasible. For larger size plants the length of the tubing would undoubtedly grow in length.

The material problems identified above are serious and need to be addressed. However, if these can be overcome, there is considerable evidence developed in this activity which is encouraging relative to the commercialization of translucent tube solar central receiver. The thermo/hydraulic analysis indicates that the translucent tubes are very efficient at absorbing the solar energy at high flux levels. If the translucent tube is compared to an opaque tube one finds that the translucent tube is considerable more efficient. For example, if an opaque tube was used with the same packing as the translucent tube the maximum tube temperature at the outlet would be about 1894°C (3442°F)! This is due to the relatively low film coefficient on the tube interior even though the packing enhances this value to a relatively high value for gas flow inside a tube. For the opaque tube all of the thermal energy that is absorbed by the tube must be transferred to the gas "through" the inside film coefficient. For the translucent tube most of the energy "by passes" this film coefficient and is radiated directly into the packing. The film coefficient and the surface area of the packing are both much higher for the packing then for the tube interior. With the unavoidable high tube temperatures for opaque tubes the radiation emission losses become extremely high for opaque tubes. For the base line translucent configuration the emission loss is about 2.4% while for an opaque tube this loss would be approximately 24%, an order of magnitude increase.

Other encouraging results of this study are the tube attachment/coupling scheme which was devised, the high design safety factors which can be achieved, and the ability to accomodate thermally induced distortions. These positive results causes one to speculate on applying the translucent tube design to point focus type receivers. For this class of solar receiver the size is usually significantly smaller than central receivers and, therefore, the required tube size is much smaller. This would allow the use of alpha-alumina tubes which are currently available.

We recommend, therefore, that investigations of applying the translucent tubes to point focus receivers be undertaken. This should, however, be preceded by a materials study to investigate the discoloration of the alpha-alumina due to exposure to high solar fluxes. This initial material study should be conducted at a solar test facility such as the Advanced Components Test Facility at The Georgia Institute of Technology. The test should consist of exposing the alpha-alumina samples to various intensities of solar flux up to about 94.6w/cm^2 (300,000 Btu/hr-ft^2). Solar transmissivity measurements should be made on the samples before the solar exposure and periodicaly during the testing. If this testing shows that the observed discoloration is not a problem then work should continue on the translucent tube concept. This work should be re-directed toward point focus type receivers.